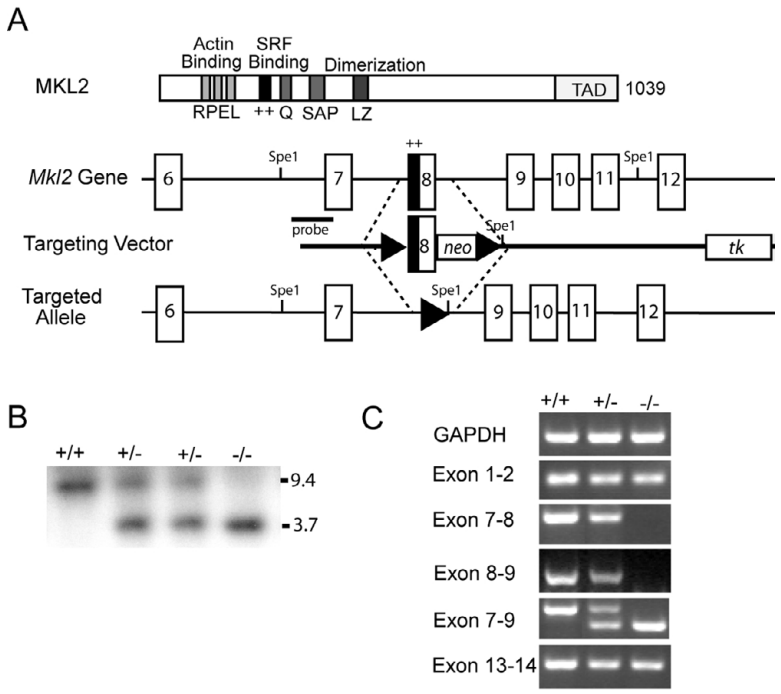

Fig. S1. Generation and characterization of *Mkl 2*$^{-/-}$ null embryos. (**A**) Schematic representation of the MKL2 protein and the gene targeting strategy used in this manuscript. The locations of the RPEL, Basic, Glutamine-rich (Q), SAP and transcriptional activation (TD) domains and leucine zipper (LZ) are shown. A schematic representation of exons 6-12 (rectangles) of the mouse *Mkl2* gene, including the location restriction enzyme sites used to genotype ES cells and mice. The position of the DNA probe used for Southern blot analysis is indicated below (black rectangle). The targeted allele contains the PGK-neomycin resistance (neo) cassette and loxP sites (triangles) flanking exon 8. (**B**) Southern blot analysis of mouse genomic DNA demonstrating the 9.4 kb wild-type allele (+) and the 3.7 kb null allele generated after Cre-mediated recombination. (**C**) PCR genotype analysis showing the expected bands corresponding to the wild-type allele (+) and conditionally targeted allele (–) following Cre-mediated recombination. PCR primers complementing the specific exons indicated are shown on the right of the ethidium bromide-stained agarose gel.

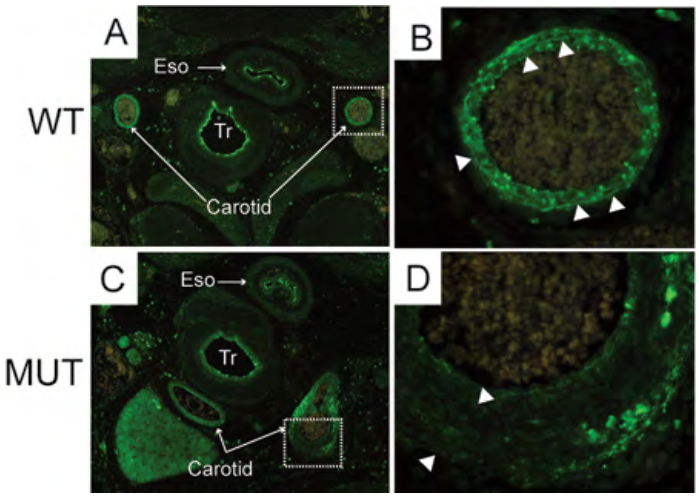

Fig. S2. Disruption of elastin organization in the carotid artery of E13.5 *Mkl2*$^{-/-}$ mutant embryos. Histological sections were prepared from E13.5 wild-type (WT) and *Mkl2*$^{-/-}$ (MUT) embryos were immunostained with anti-tropoelastin antibody (green). (**A**,**C**) Histological transverse sections cut at the level of the common carotid arteries in wild-type control (A) and *Mkl2*$^{-/-}$ mutant (MUT) embryo. The location of the trachea (Tr) and esophagus (Eso) are shown. The white rectangles indicate the sections shown in B and D. Original magnification was ×40. (**B**,**D**) High-power magnification reveals the structure of the tunica media in the left common carotid artery in a wild-type (B) and mutant (D) embryo. In the wild-type carotid, thin elastin fibers (arrows, green stain) are visualized between layers of spindle shaped vascular SMCs. By contrast, medial organization of the mutant artery is disrupted with attenuated or absence of tropoelastic staining in segments of the artery (arrows) and irregular deposition of elastin in other other segments. Original magnification was ×400.

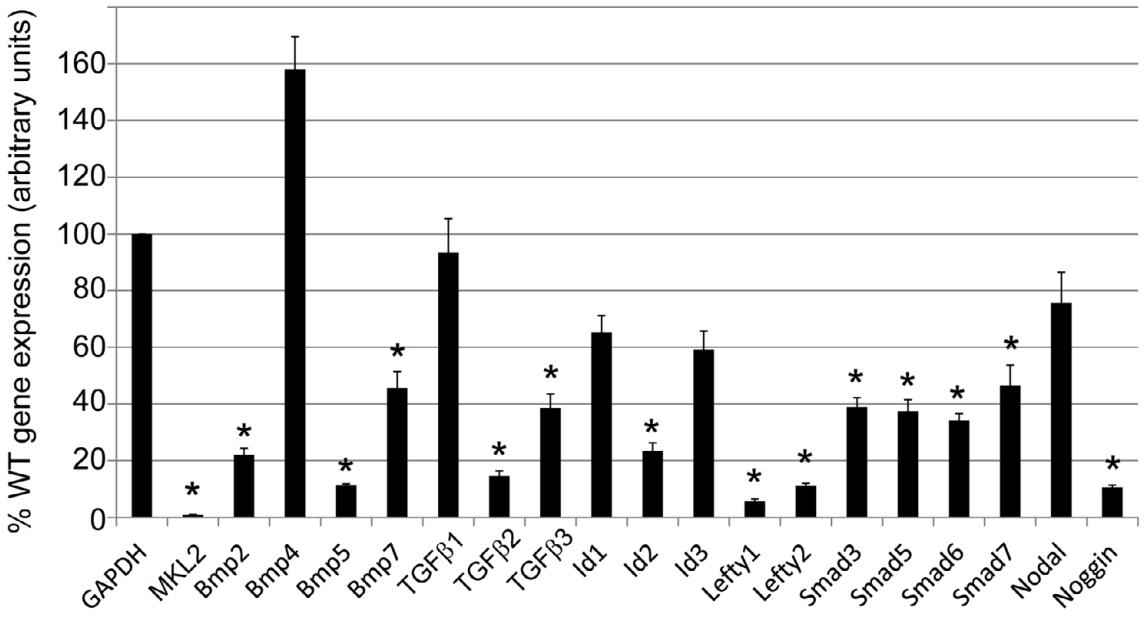

Fig. S3. Multiple TGF-β/BMP genes are downregulated in *Mkl2*$^{-/-}$ ES cells. To validate the microarray studies, qRT-PCR analyses were performed with mRNA harvested from wild-type and *Mkl2*$^{-/-}$ ES cells. The experiment was performed three times with three biological replicates used in each experiment. Data are expressed as the percentage of wild-type gene expression (arbitrary units) observed in *Mkl2*$^{-/-}$ ES cells±s.e.m. (**P*<0.01 versus wild-type gene expression).

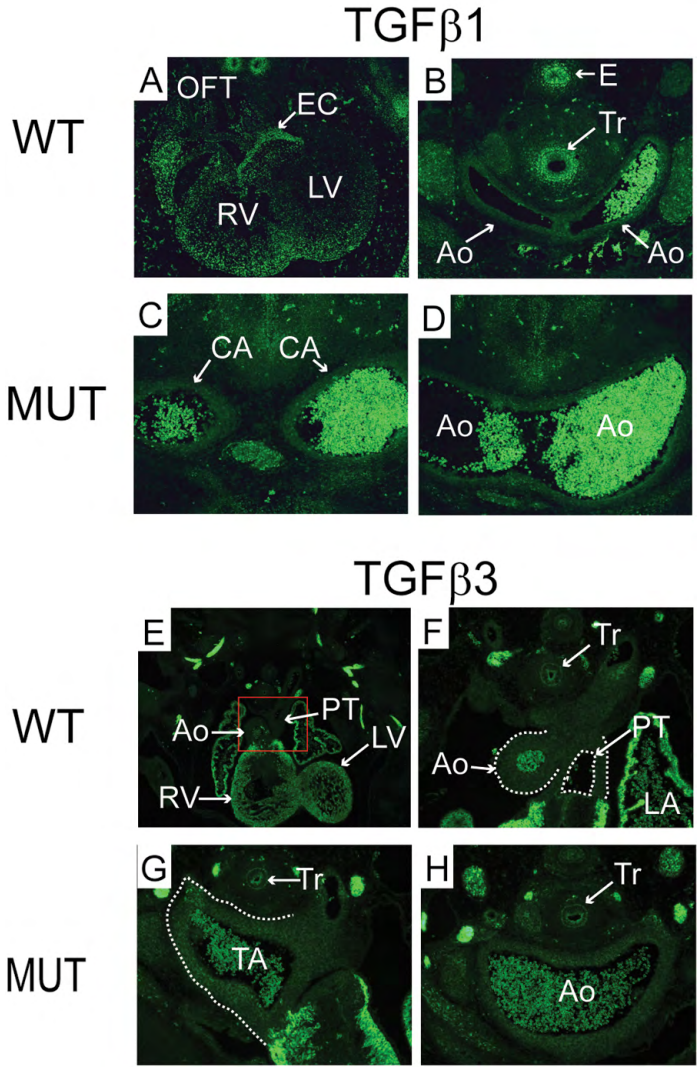

Fig. S4. Expression of TGFβ1 and TGFβ3 in the cardiac outflow tract and great arteries of E14.5 control and *Mkl2*$^{-/-}$ embryos. Histological sections cut at the level of the cardiac outflow tract of wild-type (WT) control and *Mkl2*$^{-/-}$ mutant embryos were immunostained with antibodies that recognize TGFβ1 (A-D) or TGFβ3 (E-H). (**A-D**) Abundant TGFβ1 (green stain) is observed throughout the embryonic RV and LV myocardium and endocardial cushions (EC) (A). By contrast, TGFβ1 (green stain) was expressed background levels (IgG) in the aortic arch (Ao) and carotid arteries (CA). The location of the trachea (Tr) and esophagus (E) are shown. Original magnifications were ×20 in A; ×100 in B-D. (**E**,**F**) Abundant TGFβ3 (green stain) is observed throughout the LV and RV myocardium of the control embryo. The red rectangle in E demarcates the location of F. By contrast, very low levels of TGFβ3 are observed in the ascending aorta (Ao) and pulmonary trunk (PT), whereas abundant TGFβ3 is observed in the LA. (**G**,**H**) In addition, low levels of TGFβ3 are observed in the wall of the truncus arteriosus (TA) and arch of the aorta (Ao) of *Mkl2*$^{-/-}$ mutant embryos. No appreciable difference in TGFβ3 expression was observed in the great arteries of wild-type and MUT embryos. Original magnifications were ×20 in E and ×100 in F-H.

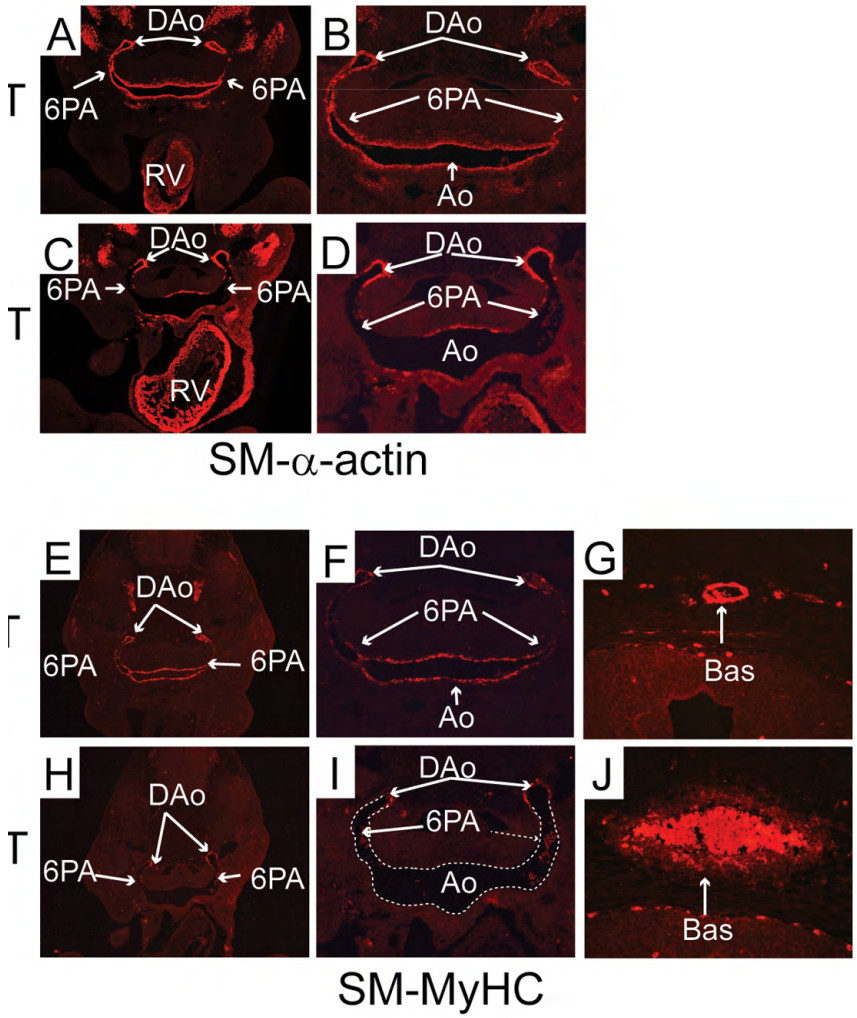

Fig. S5. Expression of SMC contractile proteins is downregulated in arteries of *Mkl2*$^{-/-}$ mutant embryos. (**A-D**) Histological sections prepared from E9.5 wild-type control (A,B) and *Mkl2*$^{-/-}$ mutant (MUT) embryos were immunostained with SM-α-actin (SMA) antibody. (A,B) Abundant SMA (red) is observed throughout the embryonic RV, pharyngeal arch arteries (6PA) and dorsal aorta (DAo) in wild-type embryos. (C,D) By contrast, expression of SMA is markedly attenuated in the pharyngeal arch arteries (6PA) and aorta (Ao) of *Mkl2*$^{-/-}$ mutant embryos. Of note, SMA expression is preserved in the dorsal aorta (DAo) and embryonic RV. Original magnifications were ×50 in A,C; ×100 in B,D. (**E-J**) Histological sections prepared from E9.5 wild-type control (E-G) and *Mkl2*$^{-/-}$ MUT (H-J) embryos were immunostained with SM-myosin heavy chain (SM-MyHC) antibody. (E,F) Abundant SM-MyC (red) is observed throughout the pharyngeal arch arteries (6PA) and dorsal aorta (DAo) in wild-type embryos. (H,I) By contrast, expression of SM-MyHC is markedly attenuated in the pharyngeal arch arteries (6PA) and aorta (Ao) of *Mkl2*$^{-/-}$ mutant embryos. Once again, SM-MyHC expression is preserved in the dorsal aorta (DAo). (G,J). Histological sections showing the basilar artery (Bas) demonstrating that expression of SM-MyHC is markedly attenuated in the mutant basilar artery (J) compared with the basilar artery in the wild-type embryo (G). Original magnifications were ×50 in E,H, ×100 in F,I and ×200 in G,J.

Table S1. PCR primers used in these studies

***Mkl2* genotyping primers**

P1	F,5'-ATACAACCCGCTTTTTAATAGG-3'
P2	F,5'-ATCTGTACAGCTTGAAACCTGGCC-3'
P3	R, 5'-TTCCCATTTCCACACGCTGATGTT-3'

qRT-PCR primers

GAPDH	F, 5'-AGTCCATGCCATCACTGCCACCCA-3' R, 5'-TCCACCACCCTGTTGCTGTAGCCG-3'
SRF	F, 5'-CCCGCTCAGACCCCACCACAGA-3' R, 5'-CAGGTAGTTGGTGATGGGGAAGGA-3'
MKL1	F, 5'-ACACTCATCAAGCAAAGCCAACCC-3', R,5'-GATCTTGGCATAGGAGGAGTCCAT-3'
MKL2	F, 5'-AACCCCTCTAACTGCAGAC-3' R,5'-GCTACGGTGTTTGTCGTTTG-3'
TGFβ1	F, 5'-ACCCTGCCCCTATATTTGGA-3', R,5'- TGGTTGTAGAGGGCAAGGAC-3'
TGFβ2	F,5'-GAACCCAAAGGGTACAATGC-3', R,5'-TGGTGTTGTACAGGCTGAGG-3'
TGFβ3	F,5'-TATGCCAACTTCTGCTCAGG-3' R,5'-CTCTGGGTTCAG GGTGTTGT-3'
SMA	F,5-'TACCATGTACCCTGGCATTGCTGA-3' R,5-'AGAAGGCCCTCTGACTTTAGAAGC-3'
SMMyHC	F, 5'-CTCTGTGCTGCACAACCTGA-3' R, 5'-TCGGCAATGGCATAGATGTG-3'
Fn	F, 5'-AGACCTGGGAAAAGCCCTACCAA-3' R, 5'-ACTGAAGCAGGTTTCCTCGGTTGT-3'
Col4a1	F, 5'-TGGATCGGCTATTCCTTCG-3' R,5'-GGCGCTTCTAAACTCTTCC-3'
Fbn1	F,5'-CTGTCCACCAGGATACTTCC-3' R,5'-CAGTGAGTTGTCGTCCATC-3'
Itgα5	F,5'-GCACCACCATTCAATTTGAC-3' R,5'-CACTGCAAGGACTTGTACTC-3'
Itgβ5	F,5'-GAATGCCTGTTGATCCACC-3' R,5'-GGATGAGGTTTGCCTTCAG-3'
Itgβ8	F,5'-CTGCAAATGTGGTCTCCTGTGC-3' R,5'-CGTTCACTTCCTGATCCACCTG-3'
Talin	F,GCTCGGGCGTTAGCAGTC-3' R,ATGGAATCTGAGACAGTCCGAGA-3'
Vinculin	F,5'-CCAAGGTCAGAGAAGCCTTCC-3' R,5'-CGTAGCTGTTCAAGGTCTGGTG-3'
Id1	F,5'-GGAGATCCTGCAGCATGTAATC-3' R,5'-ATCGTCGGCTGGAACACATG-3'
Id2	F,5'-TGGACTCGCATCCCACTATC-3' R,5'-CATTCGACATAAGCTCAGAAGG-3'

Id3	5’-GCGTGTCATAGACTACATCCTC-3’ R,5’-CCTCTTGTCCTTGGAGATCAC-3’
Bmp2	F,5’-GAATCAGAACACAAGTCA GT-3’ R,5’-GTTTGTGTTTGGCTTGACGC-3’
Bmp4	F,5’-TGTGAGGAGTTTCCATCACG-3’ R,5’-CAGCGAAGGACTGCAGGGCT-3’
Bmp5	F, 5’-GGATGGCCGCAGCATCAATGTAAA-3’ R, 5’-GAAGGCCACCATGAATGGCTGTTT-3’
Bmp7	F, 5’-ACCGCAGCCGAATTCAGGATCTAT-3’ R, 5’-TATCAAACACCAACCAGCCCTCCT-3’
Smad3	F,5’- CCAGGCTGACATGGGCAAATGAAA-3’ R, 5’-TGTCACAGTTTGCTGTGGCAATCC-3’
Smad5	F, 5’-AGCAAGAGTGTGTCAGCTCCATGA-3’ R,5’- TCCTGAAGGCTGCCAAGTAAAGGA-3’
Smad6	F, 5’-ACAAGCCACTGGATCTGTCCGATT-3’ R, 5’-AGAATTCACCCGGAGCAGTGATGA-3’
Smad7	F, 5’-TTCGGACAACAAGAGTCAGCTGGT-3’ R, 5’-AGCCTTGATGGAGAAACCAGGGAA-3’
Smad9	F,5’- TGACGGCAGGTACATTCAACCAGA-3’ R,5’- TTAAGAGCCTTGGCTTTGCTTGCC-3’
Lefty1	F,5’-ATGATTGTCAGCGTGAAGGAGGGA-3’ R,5’- TTGCATGAAAGGCACATCCTTGGG-3’
Lefty2	F,5’-TCCTGACGTATGAATGTGTGGGCA-3’ R,5’- ACTGACAATCATGGGCAAGGAGGT-3’
Nodal	F,5’- ACATGATTGTGGAGGAGTGTGGGT-3’, R,5’- TCTTTAGCTCCAGCAGGCAGAACT-3’
Noggin	F,5’-TGAGCAAGAAGCTGAGGAGGAAGT-3’ R,5’-AGGTGCACAGACTTGGATGGCTTA-3’
Pitx2	F,5’-ATG GAG ACC AAT TGT CGC AAA C-3’, R,5’-GCT TCC GTA AGG TTG GTC CAC A-3’

ChIP assay primers

Control	F,5’-ATGCTAAGTAATGGGACATTGCT-3’ R,5’-AAGTCAGCTCTGCTTCCAGG-3’
CArG1	F,5’-CTGGGGCTGACCTTGAAGGAAGAA-3’ R,5’-TTCTTCTACTCCACTGGCCCTGAG-3’
CArG2	F,5’-ATGGGGACCAAACCCAAAGGAT-3’, R,5’-ACTTCTCTACGCAAAGGGCACTG-3’
CArG3	F,5’-AAACAGTTGGGTCCCGTCCA-3’ R,5’-GAACACTATTCTGGGAGCCA,-3’
CArG4	F,5’-CTATCCCTTTCACTCCCGAGCTGTC-3’ R,5’-ACACACACACACACACACACATGAC-3’
CArG5	F,5’-GTGGTTGATTTTCATGTTGTGG-3’ R,5’-CAGAGAGTCTGCCTTTTTAGG-3’

Table S2. Primary and secondary antibodies used in these studies

Primary antibodies	**Catalog code**	**Vendor**
polyclonal anti-fibronectin	NB100-92247	Novus Biologicals
monoclonal anti-fibronectin	sc-8422	Santa Cruz Biotechnology
polyclonal anti-GAPDH	G9545	Sigma
polyclonal anti-β-tubulin	ab6046	Abcam
polyclonal anti-tropoelastin	ab21601	Abcam
monoclonal anti-phospho Smad3	CG1561	Cell Applications
monoclonal anti-TGFβ2	MAB612	R&D systems
monoclonal anti-smooth muscle-actin (1A4)	A5228	Sigma-Aldrich
polyclonal anti-phospho-paxillin (Tyr118)	2541	Cell Signaling Technology
polyclonal anti-collagen IV	AB756P	Millipore
polyclonal Anti-SRF (G20)	sc335	Santa Cruz
Rabbit IgG	2729	Cell Signaling Technology
Secondary antibodies		
Alexa Fluor® 488 Goat Anti-Mouse IgG	A-11001	Invitrogen
Alexa Fluor® 488 Rabbit Anti-Mouse IgG	A-11059	Invitrogen
Alexa Fluor® 568 Goat Anti-Rabbit IgG	A11011	Invitrogen
Alexa Fluor® 568 Goat Anti-Mouse IgG	A-11004	Invitrogen
Alexa Fluor® 594 Donkey Anti-Goat IgG (H+L)	705-585-003	Jackson ImmunoResearch
Donkey anti-mouse IgG HRP	715-035-150	Jackson ImmunoResearch

Table S3. Genes induced or repressed by twofold or more in response to *Mkl2* deletion
Owing to the small number of replicates, no statistical analysis is provided and data are regarded as exploratory

Induced genes			
Transcript cluster	**Gene symbol**	**mRNA Accession Number**	**Fold change (*Mkl2*$^{-/-}$ versus control)**
10369615	Srgn	NM_011157	30.57
10480155	Cubn	NM_001081084	7.32
10458262	Slc23a1	NM_011397	3.14
10561153	Cyp2b23	NM_001081148	3.02
10499412	Rab25	NM_016899	2.91
10446473	Lama1	NM_008480	2.74
10484276	Neurod1	NM_010894	2.34
10351368	Gpa33	NM_021610	2.20
10436978	Cbr3	NM_173047	2.16
10474575	Slc12a6	BC062099	2.02
10570516	Kbtbd11	BC080858	2.00
Repressed genes			
Transcript cluster	**Gene symbol**	**mRNA Accession Number**	**Fold change (*Mkl2*$^{-/-}$ versus control)**
10606837	Nxf3	NM_001024141	0.50
10369388	Unc5b	NM_029770	0.50
10397346	Fos	NM_010234	0.50
10454701	Wnt8a	NM_009290	0.49
10604961	Gabra3	NM_008067	0.49
10569344	Igf2	NM_001122737	0.49
10602925	Phka2	NM_172783	0.49
10359161	Soat1	NM_009230	0.49
10519951	Pion	NM_175437	0.49
10427402	Ghr	NM_010284	0.49
10408937	Atxn1	NM_009124	0.49
10377938	Eno3	NM_007933	0.48
10444258	Psmb8	NM_010724	0.48
10352320	Tmem63a	NM_144794	0.48
10503835	Rragd	NM_027491	0.48
10505132	Akap2	NM_001035533	0.48
10583203	Phxr4	BC107288	0.48
10602805	Mtap7d2	NM_001081124	0.48
10560481	Fosb	NM_008036	0.48
10347277	Igfbp2	NM_008342	0.48

10484307	Frzb	NM_011356	0.47
10513256	Lpar1	NM_010336	0.47
10406270	Glrx	NM_053108	0.47
10461629	Ms4a4d	NM_025658	0.47
10415411	Nynrin	BC057379	0.47
10545780	Exoc6b	BC145693	0.47
10599120	Dock11	NM_001009947	0.47
10571601	Pdlim3	NM_016798	0.47
10385036	Fgf18	NM_008005	0.47
10361771	Plagl1	NM_009538	0.47
10485982	Actc1	NM_009608	0.47
10442194	Zfp677	NM_172486	0.46
10604633	Cxx1b	NM_001018063	0.46
10406229	Pcsk1	NM_013628	0.46
10497817	Anxa5	NM_009673	0.46
10366546	Cpm	NM_027468	0.46
10468070	Fgf8	NM_010205	0.46
10606609	Tspan6	NM_019656	0.46
10469936	Nrarp	NM_025980	0.46
10496569	Gbp6	NM_001083312	0.46
10533050	Hspb8	NM_030704	0.46
10499132	Mab21l2	NM_011839	0.46
10543145	Thsd7a	AK173072	0.46
10406205	Erap1	NM_030711	0.45
10541524	Nanog	NM_028016	0.45
10431915	Slc38a4	NM_027052	0.45
10601980	Mum1l1	NM_175541	0.45
10359870	Pbx1	NM_183355	0.44
10505028	Slc44a1	AK141895	0.44
10496580	Gbp3	NM_018734	0.44
10576495	Trim67	BC094596	0.44
10604576	Gpc3	NM_016697	0.43
10429564	Ly6a	NM_010738	0.43
10544089	Zc3hav1	NM_028864	0.42
10449807	Abhd9	NM_001033163	0.42
10496555	Gbp1	NM_010259	0.42
10362097	H60b	AB284505	0.42
10474229	Cd59a	NM_001111060	0.42
10570957	Sfrp1	NM_013834	0.42
10534667	Serpine1	NM_008871	0.42
10464905	Npas4	NM_153553	0.41

10472688	Sp5	NM_022435	0.41
10497149	Gpr177	NM_026582	0.41
10607562	Cnksr2	NM_177751	0.41
10357137	Gli2	NM_001081125	0.40
10603208	Mid1	NM_010797	0.40
10538590	Herc5	ENSMUST00000031817	0.40
10509163	Id3	NM_008321	0.40
10496592	Gbp2	NM_010260	0.39
10603289	Clcn5	NM_016691	0.39
10352302	Lefty2	NM_177099	0.39
10438603	Igf2bp2	NM_183029	0.39
10521471	Ppp2r2c	NM_172994	0.39
10549964	Zscan4c	NM_001013765	0.38
10371379	Nuak1	NM_001004363	0.38
10544596	Tmem176b	NM_023056	0.38
10531420	Cxcl11	NM_019494	0.38
10578829	Palld	NM_001081390	0.38
10549972	Zscan4c	NM_001013765	0.38
10607587	Pdha1	NM_008810	0.37
10587639	Nt5e	NM_011851	0.37
10469167	Sfmbt2	NM_177386	0.37
10429568	Ly6c1	NM_010741	0.37
10498018	Pcdh18	NM_130448	0.36
10344966	Ly96	NM_016923	0.36
10592251	Pknox2	NM_001029838	0.36
10477920	Myl9	NM_172118	0.36
10607524	Sms	NM_009214	0.35
10361358	Rgs17	NM_019958	0.35
10583809	Cnn1	NM_009922	0.34
10604844	Sms	AF031486	0.34
10559978	Zscan4c	NM_001013765	0.34
10428619	Enpp2	NM_015744	0.34
10384223	Igfbp3	NM_008343	0.33
10407435	Akr1c18	NM_134066	0.33
10604551	Usp26	NM_031388	0.33
10445293	Pla2g7	NM_013737	0.33
10477250	Hck	NM_010407	0.32
10397984	Ppp4r4	NM_028980	0.32
10376950	Pmp22	NM_008885	0.31
10459335	Fam38b	BC147606	0.30
10360920	Tgfb2	NM_009367	0.30

10344952	Rdh10	NM_133832	0.29
10607619	Cdkl5	NM_001024624	0.29
10374777	Efemp1	NM_146015	0.28
10593123	Tagln	NM_011526	0.26
10404429	Serpinb9	NM_009256	0.26
10599348	Gria3	NM_016886	0.26
10602772	Rps6ka3	NM_148945	0.26
10467124	Acta2	NM_007392	0.26
10387855	Alox15	NM_009660	0.25
10493850	Sprr2a	NM_011468	0.23
10602977	Scml2	NM_133194	0.16
10569335	H19	NR_001592	0.15
10608138	Ddx3y	NM_012008	0.09
10608107	Uty	NM_009484	0.08
10441669	T	NM_009309	0.07
10477986	Nnat	NM_010923	0.05

Table S4. KEGG pathways repressed in response to *Mkl2* deletion by Gene Set Enrichment Analysis

KEGG pathways (From MsigDB)	Number of genes	Normalized Enrichment Score (NES)	Nominal *P* value	FDR q-val
HSA04350_TGF_BETA_SIGNALING_PATHWAY	84	-2.067	0.0000	0.0000
HSA04360_AXON_GUIDANCE	125	-1.982	0.0000	0.0021
HSA04340_HEDGEHOG_SIGNALING_PATHWAY	53	-1.942	0.0000	0.0066
HSA05217_BASAL_CELL_CARCINOMA	53	-1.900	0.0000	0.0109
HSA04510_FOCAL_ADHESION	182	-1.774	0.0000	0.0656
HSA04010_MAPK_SIGNALING_PATHWAY	231	-1.745	0.0000	0.0785
HSA04310_WNT_SIGNALING_PATHWAY	133	-1.741	0.0000	0.0696
HSA01030_GLYCAN_STRUCTURES_BIOSYNTHESIS_1	102	-1.722	0.0000	0.0754
HSA00510_N_GLYCAN_BIOSYNTHESIS	36	-1.713	0.0102	0.0725
HSA05212_PANCREATIC_CANCER	70	-1.712	0.0029	0.0661
HSA04110_CELL_CYCLE	102	-1.712	0.0014	0.0601
HSA05210_COLORECTAL_CANCER	78	-1.689	0.0014	0.0698
HSA00640_PROPANOATE_METABOLISM	30	-1.677	0.0107	0.0731
HSA04320_DORSO_VENTRAL_AXIS_FORMATION	26	-1.677	0.0101	0.0679
HSA04662_B_CELL_RECEPTOR_SIGNALING_PATHWAY	60	-1.662	0.0030	0.0741
HSA05130_PATHOGENIC_ESCHERICHIA_COLI_INFECTION_EHEC	41	-1.642	0.0114	0.0845
HSA04810_REGULATION_OF_ACTIN_CYTOSKELETON	186	-1.619	0.0026	0.0964
HSA04520_ADHERENS_JUNCTION	70	-1.618	0.0073	0.0921
HSA00760_NICOTINATE_AND_NICOTINAMIDE_METABOLISM	21	-1.612	0.0269	0.0910
HSA04916_MELANOGENESIS	89	-1.596	0.0088	0.0999
HSA05131_PATHOGENIC_ESCHERICHIA_COLI_INFECTION_EPEC	41	-1.589	0.0144	0.1018
HSA00410_BETA_ALANINE_METABOLISM	24	-1.589	0.0339	0.0975
HSA00563_GLYCOSYLPHOSPHATIDYLINOSITOL_ANCHOR_BIOSYNTHESIS	19	-1.586	0.0204	0.0963
HSA00100_BIOSYNTHESIS_OF_STEROIDS	22	-1.558	0.0383	0.1162
HSA04530_TIGHT_JUNCTION	114	-1.555	0.0055	0.1147
HSA00561_GLYCEROLIPID_METABOLISM	46	-1.533	0.0411	0.1316
HSA05220_CHRONIC_MYELOID_LEUKEMIA	71	-1.532	0.0177	0.1281
HSA00512_O_GLYCAN_BIOSYNTHESIS	28	-1.521	0.0369	0.1339
HSA04620_TOLL_LIKE_RECEPTOR_SIGNALING_PATHWAY	88	-1.511	0.0226	0.1399
HSA04060_CYTOKINE_CYTOKINE_RECEPTOR_INTERACTION	208	-1.510	0.0063	0.1359
HSA00280_VALINE_LEUCINE_AND_ISOLEUCINE_DEGRADATION	40	-1.505	0.0305	0.1361
HSA01031_GLYCAN_STRUCTURES_BIOSYNTHESIS_2	51	-1.501	0.0250	0.1358
HSA05221_ACUTE_MYELOID_LEUKEMIA	49	-1.495	0.0363	0.1383
HSA04150_MTOR_SIGNALING_PATHWAY	42	-1.493	0.0422	0.1361
HSA05010_ALZHEIMERS_DISEASE	27	-1.462	0.0677	0.1653
HSA05211_RENAL_CELL_CARCINOMA	67	-1.459	0.0427	0.1631

HSA00380_TRYPTOPHAN_METABOLISM	50	-1.456	0.0541	0.1626
HSA00530_AMINOSUGARS_METABOLISM	26	-1.447	0.0689	0.1687
HSA04115_P53_SIGNALING_PATHWAY	57	-1.439	0.0365	0.1754
HSA00252_ALANINE_AND_ASPARTATE_METABOLISM	29	-1.433	0.0733	0.1770
HSA04660_T_CELL_RECEPTOR_SIGNALING_PATHWAY	89	-1.425	0.0418	0.1832
HSA00230_PURINE_METABOLISM	137	-1.409	0.0332	0.1976
HSA00120_BILE_ACID_BIOSYNTHESIS	31	-1.381	0.0983	0.2312
HSA00251_GLUTAMATE_METABOLISM	30	-1.378	0.0992	0.2301
HSA00650_BUTANOATE_METABOLISM	42	-1.378	0.0970	0.2251
HSA04120_UBIQUITIN_MEDIATED_PROTEOLYSIS	34	-1.376	0.0902	0.2239
HSA04930_TYPE_II_DIABETES_MELLITUS	41	-1.375	0.0927	0.2197
HSA00600_SPHINGOLIPID_METABOLISM	33	-1.374	0.1128	0.2168
HSA00020_CITRATE_CYCLE	25	-1.363	0.1036	0.2261
HSA03320_PPAR_SIGNALING_PATHWAY	57	-1.356	0.0922	0.2324
HSA04330_NOTCH_SIGNALING_PATHWAY	39	-1.346	0.1049	0.2411
HSA04130_SNARE_INTERACTIONS_IN_VESICULAR_TRANSPORT	30	-1.345	0.1197	0.2373
HSA04920_ADIPOCYTOKINE_SIGNALING_PATHWAY	68	-1.342	0.0708	0.2370
HSA00340_HISTIDINE_METABOLISM	36	-1.336	0.1130	0.2405
HSA04630_JAK_STAT_SIGNALING_PATHWAY	132	-1.326	0.0523	0.2493